Toggle involving *cis*-interfering noncoding RNAs controls variegated gene expression in yeast

Stacie L. Bumgarner[a], Robin D. Dowell[b], Paula Grisafi[a], David K. Gifford[b,1], and Gerald R. Fink[a,1]

[a]Whitehead Institute for Biomedical Research, 9 Cambridge Center, Cambridge, MA 02142; and [b]Computer Science and Artificial Intelligence Laboratory, Massachusetts Institute of Technology, 32 Vassar Street, Cambridge, MA 02139

Contributed by Gerald R. Fink, August 26, 2009 (sent for review July 24, 2009)

The identification of specific functional roles for the numerous long noncoding (nc)RNAs found in eukaryotic transcriptomes is currently a matter of intense study amid speculation that these ncRNAs have key regulatory roles. We have identified a pair of *cis*-interfering ncRNAs in yeast that contribute to the control of variegated gene expression at the *FLO11* locus by implementing a regulatory circuit that toggles between two stable states. These capped, polyadenylated ncRNAs are transcribed across the large intergenic region upstream of the *FLO11* ORF. As with mammalian long intervening (li)ncRNAs, these yeast ncRNAs (*ICR1* and *PWR1*) are themselves regulated by transcription factors (Sfl1 and Flo8) and chromatin remodelers (Rpd3L) that are key elements in phenotypic transitions in yeast. The mechanism that we describe explains the unanticipated role of a histone deacetylase complex in activating gene expression, because Rpd3L mutants force the ncRNA circuit into a state that silences the expression of the adjacent variegating gene.

FLO11 | intergenic transcription | Rpd3L histone deacetylase | transcriptional interference | regulatory RNAs

Recent genome-wide studies of eukaryotic transcriptional landscapes in yeast, mice, and humans have revealed extensive activity in regions previously expected to be transcriptionally inert (1–13). A subset of these noncoding (nc)RNAs are long ncRNAs transcribed across intergenic regions. In mammalian cells, transcription of numerous such long intervening (li)ncRNAs is regulated by the binding of transcription factors critical to mammalian development, including Oct4, Nanog, and Sox2 (5). This observation has engendered speculation that mammalian lincRNAs have key roles in development by regulating expression of protein-coding ORFs via mechanisms distinct from the Dicer-dependent RNAi pathway (5, 14–16). However, experiments that would conclusively test the postulated roles for the vast majority of eukaryotic long ncRNAs have not yet been performed (5). Careful interrogation of specific loci is necessary to distinguish between ncRNAs that represent mere transcriptional "noise" and those that have a bona fide role in regulation and development (17–22). Long intergenic ncRNAs also exist in yeast, and despite the tractability of this model system, most remain uncharacterized.

Recent studies of an intergenic ncRNA that regulates the *SER3* gene (23, 24), and other subsequent investigations at specific genes in yeast (25–27), have begun to reveal mechanisms, alternative to the RNAi pathways, via which ncRNAs regulate the expression of protein-coding ORFs. The detection in genome-wide studies of noncoding transcripts within promoter regions and numerous instances of overlapping complementary transcripts points to additional regulatory roles for yeast ncRNAs (2, 3, 8–11).

We have identified a pair of long *cis*-interfering ncRNAs in yeast that contribute to the control of gene expression at the *FLO11* locus via a previously uncharacterized type of regulatory circuit, in which these ncRNAs toggle to control transcription of the downstream protein-coding ORF. Transcription of these yeast ncRNAs is regulated by transcription factors Sfl1 and Flo8, key players in *FLO11*-dependent developmental transitions that enable this organism to adapt to changing environments (28–35).

Functional characterization of the circuitry involving this pair of ncRNAs helps to explain two puzzling phenomena. First, *FLO11* is expressed in a binary or "variegated" fashion in clonal populations of WT cells: *FLO11* is transcribed at high levels ("on") in some cells and is completely transcriptionally silenced ("off") in others (35). In this report, we present evidence that these ncRNAs contribute to the variegated expression observed at *FLO11* by toggling between the transcription of one or the other of these ncRNAs. Second, Rpd3L, a histone deacetylase (HDAC), has an unanticipated net activating effect on *FLO11* transcription. This paradox is unresolved in the literature. At some gene targets, Rpd3L displays the net repressive effect on transcription expected of an HDAC (36–38), but at others, it has an unexpected net activating effect on transcription (39–42). In this report, we demonstrate that Rpd3L activates *FLO11* transcription via its repressive effects on one of the *cis*-acting ncRNAs that itself negatively regulates *FLO11* transcription. Because it was the paradoxical role of Rpd3L as an activator of *FLO11* transcription that led us to the discovery of the ncRNAs at the *FLO11* locus, our presentation of experimental results begins there.

Results

HDAC Rpd3L Is a Net Activator of *FLO* Gene Expression. Null mutations (Rpd3L$^-$) in components of Rpd3L, including Cti6, Rxt2, and Pho23, result in increased silencing of the *FLO11* and *FLO10* promoters, indicating that Rpd3L is a net transcriptional activator of these genes. This role for Rpd3L is demonstrated in three ways. First, promoter activity was assayed in strains in which the endogenous promoter is fused to a reporter gene (P_{FLO11}-*URA3*, Fig. 1*A*; P_{FLO11}-*GFP* or P_{FLO10}-*GFP*; Fig. S1*A*), which precisely replaces the *FLO* ORF (Table S1). Detection of ura$^-$ (5-FOA resistant) or gfp$^-$ cells in WT vs. Rpd3L$^-$ strains indicates that *FLO* promoter silencing is elevated in Rpd3L$^-$ cell populations. Second, Northern blot analysis (Fig. 1*B*) shows that *FLO11* mRNA is reduced in Rpd3L$^-$ (*cti6*) compared with WT. Third, disruption of Rpd3L function results in loss of *FLO11*-dependent phenotypes. Homozygous Rpd3L$^-$ diploids fail to form pseudohyphae (Fig. 1*C*) and Rpd3L$^-$ haploids do not adhere to YPD agar (Fig. 1*D*). These phenotypes are observed in *rpd3*Δ deletion mutants, indicating that the catalytic component of the Rpd3L HDAC is required for net activation of *FLO11*. Rpd3L$^-$ strains transformed with a P_{TEF}-*FLO11* plasmid

Author contributions: S.L.B., R.D.D., P.G., D.K.G., and G.R.F. designed research; S.L.B., R.D.D., and P.G. performed research; S.L.B., R.D.D., P.G., and D.K.G. contributed new reagents/analytic tools; S.L.B., R.D.D., P.G., D.K.G., and G.R.F. analyzed data; and S.L.B. and G.R.F. wrote the paper.

The authors declare no conflict of interest.

See Commentary on page 18049.

[1]To whom correspondence may be addressed. E-mail: gfink@wi.mit.edu or gifford@mit.edu.

This article contains supporting information online at www.pnas.org/cgi/content/full/0909641106/DCSupplemental.

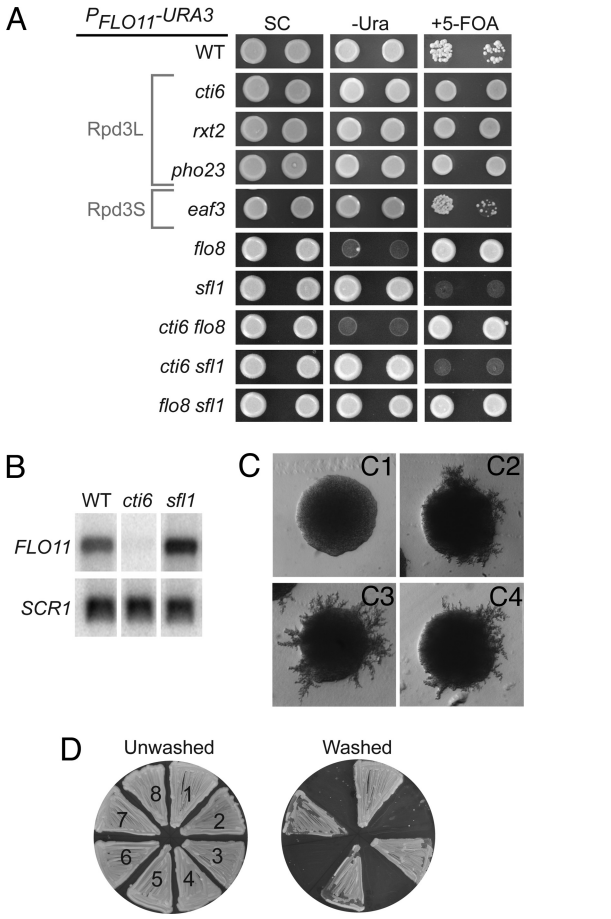

Fig. 1. The HDAC Rpd3L is a net activator of *FLO11* transcription. (*A*) *FLO11* promoter activity was assayed in haploids containing the P_{FLO11}-*URA3* reporter at the endogenous locus. Four-fold serial dilutions were spotted onto SC, -Ura, and 5-FOA (0.1%) media. Cells with active *FLO11* promoters are Ura^+ and $5\text{-}FOA^S$, whereas silenced cells are Ura^- and $5\text{-}FOA^R$. (*B*) Northern blot analysis with a probe for *FLO11* (3502–4093 bp) shows that reporter assays reflect average steady-state *FLO11* mRNA levels. (*C*) Pseudohyphal growth is lost in $Rpd3L^-$ diploids, but is restored by P_{TEF}-*FLO11* on a 2-μ plasmid. *C1*, *cti6*/*cti6* + vector; *C2*, *cti6*/*cti6* + P_{TEF}-*FLO11*; *C3*, WT + vector; *C4*, WT + P_{TEF}-*FLO11*. (*D*) Loss of Rpd3L function abolishes haploid adhesion. The same plate, before (*Left*) and after (*Right*) washing, is shown. P_{TEF}-*FLO11* on a 2-μ plasmid restores adhesion. (part 1) WT; (part 2) *flo11*; (part 3) *cti6* + P_{TEF}-*FLO11*; (part 4) *cti6* + vector; (part 5) *rxt2* + P_{TEF}-*FLO11*; (part 6) *rxt2* + vector; (part 7) *rpd3* + P_{TEF}-*FLO11*; (part 8) *rpd3* + vector.

recover both diploid filamentation and haploid adhesion (Fig. 1 *C* and *D*), demonstrating that the phenotypic defects observed in $Rpd3L^-$ strains are a direct consequence of their loss of *FLO11* expression. These phenotypes are specific to the Rpd3L and not the Rpd3S complex. *FLO11* promoter activity is not affected in a strain lacking Eaf3 (Fig. 1*A*), unique to Rpd3S (36, 43). Experiments described below use null alleles of Cti6, unique to Rpd3L, to assay the effects of disrupting Rpd3L function.

Epistasis data suggest that (*i*) Rpd3L works upstream of *FLO*-specific transcription factors Sfl1 (repressor) (31, 33, 44) and Flo8 (activator) (28, 29,33); and (*ii*) net activation of *FLO11* by Rpd3L depends on Sfl1 function. The phenotype of the $Rpd3L^-$ *sfl1* double mutant is indistinguishable from that of the *sfl1* mutant, in which *FLO11* promoter silencing is lost in all cells (Fig. 1*A*) (25). As in the *flo8* strain, all cells have a silenced *FLO11* promoter in the $Rpd3L^-$ *flo8* double mutant (Fig. 1*A*). *SFL1* mRNA levels in $Rpd3L^-$ mutant strains do not differ significantly from WT (Fig. S1*B*), indicating that the role of Rpd3L in activating *FLO11* expression is not via an indirect mechanism involving transcriptional repression of *SFL1*.

Rpd3L Localization to the *FLO11* Promoter Alters Transcription Factor Binding and Chromatin Remodeling. Genome-wide ChIP-chip detects Rpd3 localization at two regions within the upstream intergenic region of *FLO11*: ~1,250 and ~2,850 bp upstream of the ATG of *FLO11* (Fig. 2*A*). Gene-specific ChIP shows that enrichment of Rpd3 upstream of *FLO11* is at least 4-fold higher than at unbound regions, and exceeds enrichment at the *INO1* promoter (Fig. 2*A* and Fig. S2*A*), where Rpd3 localization is reported (45).

Compared with WT, localization of the transcriptional activator Flo8 to the *FLO11* promoter is significantly decreased in the $Rpd3L^-$ mutant and, as previously reported (33), is increased in *sfl1* (Fig. 2*B*). In the $Rpd3L^-$ *sfl1* double mutant, Flo8 binding is restored, but not to the levels observed in *sfl1*. Thus, Flo8 binding remains impaired in the $Rpd3L^-$ mutant even in the absence of Sfl1. Yeast TATA box-binding protein (TBP) localization to the *FLO11* TATA box (−92 bp) is absent in $Rpd3L^-$ and is elevated above WT levels in *sfl1* (Fig. 2*C*). Histone H4 localization shows that nucleosome eviction fails to occur at the *FLO11* core promoter in $Rpd3L^-$ cells compared with *sfl1* cells (Fig. 2*D*). Differential enrichment of TBP and H4 is not merely an artifact of differential overall signal on the arrays, because signal is similar at control regions (Fig. S2 *C* and *D*).

Rpd3L, Sfl1, and Flo8 Control a Pair of *cis*-Acting ncRNAs, Implementing a Toggle That Contributes to *FLO11* Regulation. The findings that Rpd3L localizes to the *FLO11* promoter and activates *FLO11* expression presented a paradox, because HDACs normally function as repressors of transcription by condensing chromatin (46). This paradox could be resolved if Rpd3L repressed the transcription of a *cis*-acting ncRNA, itself responsible for repression of *FLO11* transcription via a promoter occlusion mechanism (23, 24). To test this possibility, we assayed for polyadenylated transcripts deriving from the ~3.6-kb region upstream of *FLO11*. Strand-specific microarrays provided an initial view of transcription surrounding the *FLO11* locus. These arrays detected Crick- and Watson-strand noncoding transcription (no ORFs >303 bp; Fig. S3*A*) across several kilobases of the upstream intergenic region of *FLO11* (Fig. 3*A*). An analogous result was observed at the variegating *FLO10* locus (Fig. S3*B*) (35).

To quantify and determine the size of the ncRNAs upstream of *FLO11*, Northern blot analysis was performed on oligo(dT)-selected RNAs with strand-specific RNA probes (Fig. 3 *B*–*D*). Probes for Crick-strand transcription detect a ~3.2-kb ncRNA, designated *ICR1* (interfering Crick RNA), transcribed across much of the upstream intergenic region of *FLO11* (Fig. 3*C*). Low levels of an ~8-kb Crick-strand transcript, which may represent a species transcribed across the *FLO11* promoter and ORF, are also detected in some mutants (Fig. 3 *C* and *D*). A probe specific for Watson-strand transcription at a region far upstream of the *FLO11* ORF detects another ncRNA, ~1.2 kb in length and designated *PWR1* (promoting Watson RNA) (Fig. 3*C*).

Cap-dependent RACE was used to map the 5′ and 3′ ends of *ICR1* and *PWR1*. The 5′ RACE identified start sites for *ICR1* over a 250-bp range, 3,445–3,197 bp upstream of *FLO11* (Fig. 3*B* and Table S2). The 3′ RACE identified a strong stop site for *ICR1* 209 bp upstream of *FLO11* and other stops closer to (6, 4, and 2 bp upstream) and within (+10 and +24 bp) the *FLO11* ORF itself (Fig. 3*B* and Table S2). The 5′ RACE for *PWR1* identified start sites over a 160-bp range, 2,190 to 2,339 bp upstream of *FLO11* (Fig. 3*B* and Table S3). *PWR1* is complementary to ~1.2 kb of the 5′ end of *ICR1* and terminates in the region where *ICR1* initiates, between 3246 and 3409 bp upstream of *FLO11* (Fig. 3*B* and Table S3). This configuration suggests

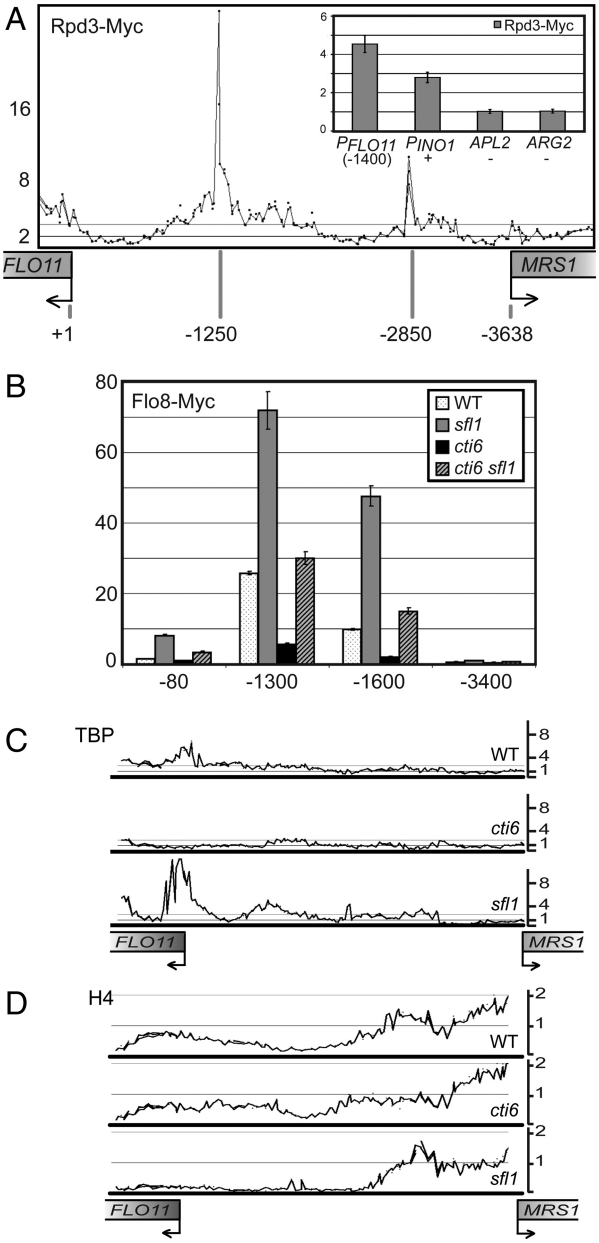

Fig. 2. Rpd3L localization to the *FLO11* promoter alters transcription factor binding and chromatin remodeling. (*A*) ChIP-chip experiments were performed using a functional Myc-tagged allele of Rpd3 in a WT haploid (Fig. S2*B*). The plot shows fold enrichment of Rpd3-Myc in chromatin immunoprecipitated (IP) with an anti-Myc antibody normalized to the whole-cell extract (WCE). (*Inset*) Quantitative PCR was performed on IP and WCE using primers specific for the *FLO11* promoter (−1,400 bp), for positive binding control P_{INO1}, and for unbound regions *APL2* and *ARG2*. Data were normalized to unbound region *ARK1* and are expressed as fold enrichment ± SD. (*B*) Localization of Flo8 using a Myc-tagged allele in WT and mutant haploids was assayed by qPCR with primers specific for the *FLO11* promoter on IP (anti-Myc) and WCE. Data were normalized to unbound region *ACT1* and are expressed as fold enrichment ± SEM. (*C*) Localization of TBP was assayed by ChIP-chip in haploid WT, *cti6*, and *sfl1* cells. The plot shows fold enrichment of TBP at the *FLO11* promoter in IP (anti-TBP) normalized to WCE. (*D*) Localization of histone H4 was assayed by ChIP-chip in haploid WT, *cti6*, and *sfl1* cells. The plot shows fold enrichment of H4 at the *FLO11* promoter in IP (anti-H4) normalized to WCE.

possible regulatory roles for *ICR1* and *PWR1* (23–25): *ICR1* could repress *FLO11* transcription by occluding its promoter, whereas *PWR1* could promote *FLO11* transcription by interfering with *ICR1*

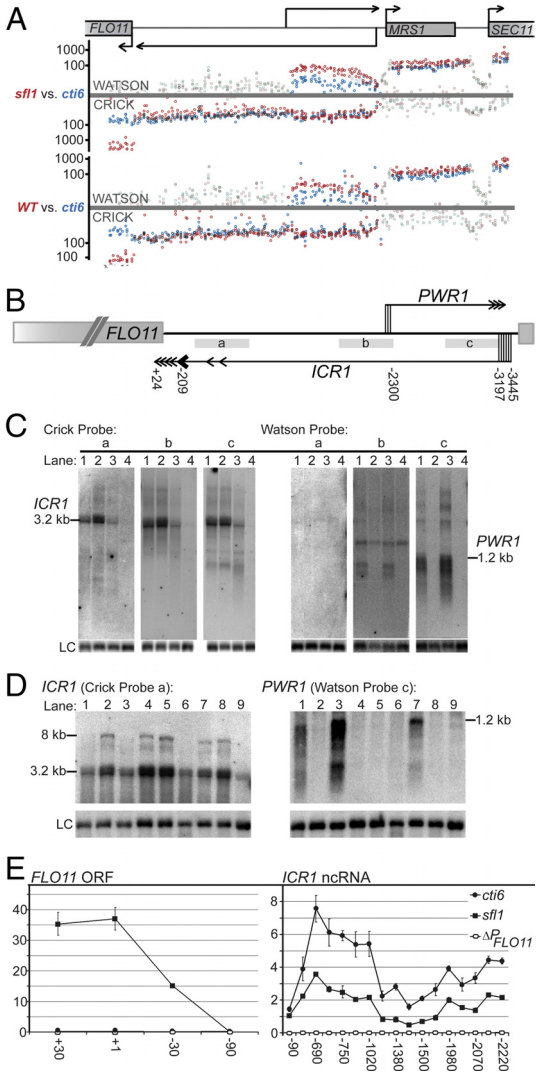

Fig. 3. Rpd3L, Sfl1, and Flo8 control a pair of ncRNAs transcribed upstream of *FLO11*. (*A*) Genome-wide transcription of polyadenylated [poly(A)] RNAs was profiled in haploid WT, Rpd3L⁻ (*cti6*), and *sfl1* strains with strand-specific microarrays. Transcription detected near the *FLO11* locus is shown. In the plots, each circle represents a probe with log signal intensity indicated on the *y* axis. Circles positioned above each *x* axis indicate Watson-strand transcription. Circles positioned below each *x* axis indicate Crick-strand transcription. Results from two arrays are shown. (*Upper*) Transcription in *sfl1* (red circles) vs. *cti6* (blue circles); (*Lower*) Transcription in WT (red circles) vs. *cti6* (blue circles). Faded circles represent probes that were not called as part of a transcript in the analysis. A larger version of these plots is provided in Fig. S3. (*B*) Map of ncRNAs detected upstream of *FLO11* and probes used in Northern blot analysis. Probes a, b, and c hybridize to regions located 284–819, 1653–2255, and 2631–3226 bases upstream of *FLO11*, respectively. Vertical lines at the 5′ ends of *ICR1* and *PWR1* ncRNAs show the range of start sites identified by RACE (Tables S2 and S3). Arrowheads at the 3′ ends of the ncRNAs indicate the range of stop sites identified by RACE (Tables S2 and S3). (*C*) Northern blot analysis was performed on poly(A) RNA from haploid WT (lane 1), *cti6* (lane 2), *sfl1* (lane 3), and ΔP_{FLO11} (lane 4) where the entire intergenic region upstream of *FLO11* is deleted. *FLO11* is, by convention, encoded on the Crick strand; other transcripts encoded on this strand are designated ''Crick-strand,'' and those encoded on the complementary strand are designated ''Watson-strand.'' Crick-strand specific probes 1–3 detect the ~3.2-kb *ICR1* ncRNA. Watson-strand specific probes 2 and 3 detect a diffuse band with upper size of ~1.2 kb representing the ncRNA *PWR1*. Load control (LC) = *SCR1*. (*D*) Northern blot analysis was performed on poly(A) RNA from haploid WT (lane 1), *cti6* (lane 2), *sfl1* (lane 3), *flo8* (lane 4), *cti6 flo8* (lane 5), *sfl1 flo8* (lane 6), *cti6 sfl1* (lane 7), *cti6 sfl1 flo8* (lane 8), and ΔP_{FLO11} (lane 9). LC = *rRNA*. (*E*) Quantitative PCR assay of transcription using primers tiled from +120 bp within the *FLO11* ORF to 2280 bp upstream was performed for *cti6*, *sfl1*, and ΔP_{FLO11} haploids. Detected transcription normalized to *SCR1* levels is presented ±SD.

transcription. The analogous pair of ncRNAs transcribed upstream of *FLO10* (Fig. S3) adds support to this model.

There is an inverse correlation observed between *ICR1* and *PWR1* transcription. *ICR1*, but not *PWR1*, is transcribed at the highest levels detected in this study in mutants (Rpd3L$^-$, *flo8*, Rpd3L$^-$ *flo8*, Rpd3L$^-$ *flo8 sfl1*; Fig. 3 *C* and *D*) where transcription of *FLO11* is largely silenced. These data implicate Flo8 and Rpd3L as repressors of *ICR1*. *ICR1* is barely detectable in *sfl1* mutants in which Rpd3L function is still intact, indicating that Sfl1 function normally promotes *ICR1* transcription. *PWR1* is detected only in the strains in which *FLO11* is also transcribed at high levels (Figs. 1 *A* and *B* and 3 *C* and *D*). *PWR1* transcription requires Flo8 and is promoted by Rpd3L activity, but is repressed by Sfl1 function (Fig. 3 *C* and *D*). Both *PWR1* and *ICR1* are detected in the mixed population of *FLO11* on and off cells in the variegating WT strain (Fig. 3*C*). Quantitative (q)PCR assays support the presence of the *ICR1* transcript, the quantitative differences in its transcription observed by Northern blot analysis, and an inverse correlation between *ICR1* and *FLO11* transcription (Fig. 3*E* and Fig. S4*A*).

If *ICR1* transcription across the *FLO11* promoter has a causal role in repressing *FLO11*, then termination of the *ICR1* transcript should block this inhibition and restore *FLO11* expression. This prediction was tested with strains in which *ICR1* is terminated by constructs (*T1–T3*) containing a transcriptional terminator (Fig. 4*A*). The control construct (*C*) contains an ORF sequence with no terminator (Fig. 4*A*). Insertion of *T1*, *T2*, or *T3* at a site 3,041 bp upstream of *FLO11* (~350 bp downstream of *ICR1* initiation) restores *FLO11*-dependent adhesion in Rpd3L$^-$ mutants (Fig. 4*D*). The extent of rescue correlates directly with the strength of the terminator (Fig. 4*C*) and the resulting increase in *FLO11* expression (Fig. 4*B*). Control construct *C* inserted at the same site does not terminate *ICR1* and does not restore adhesion to the Rpd3L$^-$ mutant (Fig. 4 *B–D*).

ICR1 and *PWR1* show evidence of reciprocal transcriptional interference. This interference is suggested by the inverse correlation in their transcription and by Northern blot bands indicative of a range of transcript sizes that could result from interference (Fig. 3 *C* and *D*). A genomic comparison of four yeasts closely related to *Saccharomyces cerevisiae* (49, 50) shows that the region of overlap between *PWR1* and *ICR1* represents the least conserved DNA sequence in this region, suggesting that transcription per se, rather than specific DNA sequence, is important there (Fig. S4*B*). A *URA3* gene inserted as a surrogate-initiated similarly to *ICR1* revealed *PWR1*-imposed interference on *URA3* expression (Fig. S5). Last, termination of *ICR1* increases *PWR1* levels in the Rpd3L$^-$ background (Fig. 4*C*). The fact that low level *ICR1* is detected even in *sfl1* mutants (Fig. 3 *C* and *D*) suggests that *ICR1* may be constitutive, supporting a model in which its levels are tuned by *PWR1* transcription.

The insertion of a terminator into just one copy of the *FLO11* promoter in Rpd3L$^-$ diploids up-regulates expression of the downstream ORF only in *cis* (Fig. 4*E*). Overexpression of *ICR1* or *PWR1* in *trans* has no effect on *FLO11* promoter activity in WT, *sfl1*, *flo8*, or Rpd3L$^-$ strains (Fig. S6). These results show that *ICR1* and *PWR1* function in *cis* to regulate *FLO11* transcription.

Together, these data support a mutual interference between *PWR1* and *ICR1*, and suggest a model for transcriptional variegation at the *FLO11* locus involving a toggle between these ncRNAs (Fig. 5).

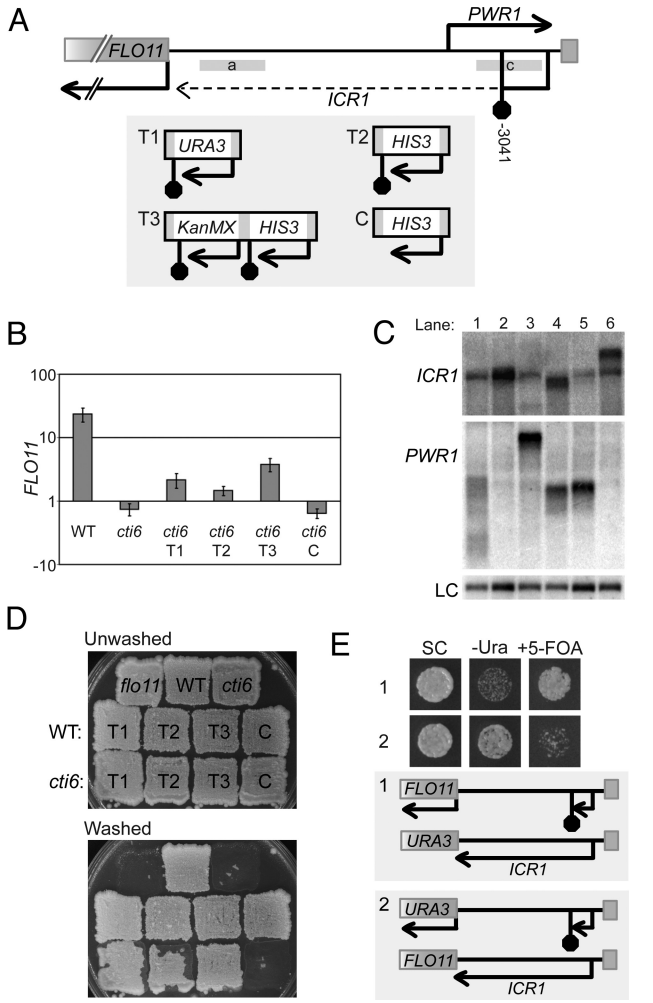

Fig. 4. *ICR1* represses *FLO11* transcription in *cis*. (*A*) Schematic representation of transcriptional terminator constructs *T1*, *T2*, and *T3* and control construct *C* inserted −3,041 bp upstream of *FLO11*. *T1*, *Kluyveromyces lactis URA3* expressed under its own promoter and followed by its terminator (47); *T2*, *S. cerevisiae HIS3* gene with its terminator (+1 to +817) (23); *T3*, *HIS3* gene and its terminator followed by *KanMX* and the *TEF* terminator (48); *C*, *HIS3* ORF (+1 to +663, no terminator) (23). (*B*) Quantitative PCR assay of *FLO11* transcript levels was performed in haploid WT and Rpd3L$^-$ (*cti6*) strains in which *T1*, *T2*, *T3*, or *C* was inserted (with no loss of endogenous sequence) 3,041 bp upstream of *FLO11*. *FLO11* levels normalized to *ACT1* are presented ± SD. (*C*) *ICR1* and *PWR1* levels were assayed by Northern blot analysis using strand-specific probes a and c, respectively. Strains: WT (lane 1); *cti6* (lane 2); *cti6* + *T1* (lane 3); *cti6* + *T2* (lane 4); *cti6* + *T3* (lane 5); and *cti6* + *C* (lane 6). Termination of *ICR1* by *T1*, *T2*, or *T3* increases *PWR1* transcription. The larger *PWR1* band in lane 3 is the size predicted due to insertion of *T1* (1.4 kb) if the *K. lactis URA3* terminator is unidirectional. The shorter *PWR1* transcripts in lanes 4 and 5 suggest that the *HIS3* terminator in the *T2* and *T3* constructs is bidirectional. (*D*) Haploid adhesion to YPD agar was assayed. The same plate, before (*Upper*) and after (*Lower*) washing, is shown. (*E*) In *MATa*/*MATa cti6*/*cti6* diploids with one allele of *FLO11* intact and the other precisely replaced by the *URA3* reporter gene, insertion of *T3* 3,041 bp upstream restores expression of the downstream ORF only in *cis*. *MATa*/*MATa* diploids were used because *FLO11* expression is dramatically reduced in *MATa*/*MATα* diploids compared with haploids (51).

Discussion

We report the discovery of two long intergenic ncRNAs, *ICR1* and *PWR1*, that have key roles in regulating transcription of the nearby protein-coding ORF *FLO11*. The ~3.2-kb *ICR1* ncRNA is initiated far upstream (~3.4 kb) from the *FLO11* ORF and is transcribed across much of the large promoter of *FLO11* (53), repressing *FLO11* transcription in *cis*. Our data support a "promoter occlusion" model (23, 24), in which transcription of *ICR1* blocks access to general transcription factors and to chromatin remodelers required for nucleosome ejection. The ~1.2-kb *PWR1* ncRNA is transcribed from the strand complementary to that encoding *ICR1*, and promotes *FLO11* transcription by interfering with *ICR1*.

In our model (Fig. 5), the competitive binding of Sfl1 or Flo8 at their respective binding domains (33) initiates events that

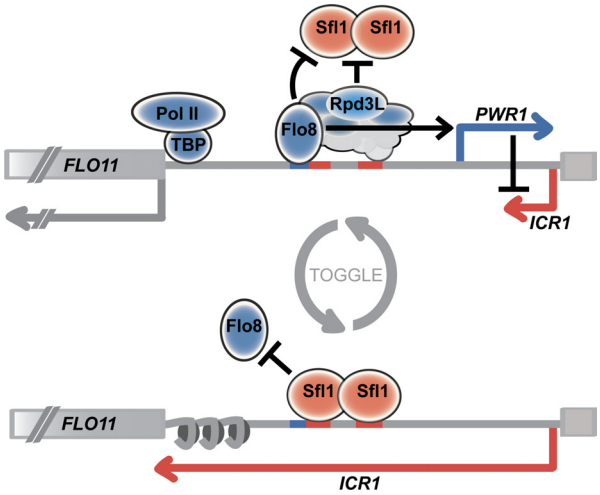

Fig. 5. Model for transcriptional variegation at the *FLO11* locus involving a toggle between the ncRNAs *ICR1* and *PWR1*. Competitive binding of Sfl1 or Flo8 at their respective binding domains [indicated by a blue line (for Flo8) or red lines (for Sfl1) on the DNA] (33) initiates events that contribute to either (*i*) a switch to the silenced *FLO11* state (Sfl1-binding) or (*ii*) a switch to the competent state (Flo8 binding). Competition between Sfl1 and Flo8 determines which of two mutually exclusive ncRNA transcription programs occurs. *ICR1* represses *FLO11* transcription, whereas *PWR1* promotes it. Localized chromatin condensation by Rpd3L at an upstream site (~1,250 bp; Fig. 2*A*) could hinder the access of Sfl1 to its binding site, but promote Flo8 binding, toggling the *FLO11* promoter toward a state competent for transcription of the protein-coding ORF.

contribute to either (*i*) stabilization of the silent state (Sfl1 binding) or (*ii*) stabilization of the competent state (Flo8 binding) in each cell. Competition between Sfl1 and Flo8 determines which of two mutually exclusive ncRNA transcription programs occurs. Lack of *PWR1* transcription in the absence of Flo8 allows transcription of *ICR1* to occlude downstream sequences that recruit other *trans*-activators of *FLO11* expression. Reciprocally, the absence of Sfl1 binding allows Flo8 binding and *PWR1* transcription that interferes with *ICR1*, preventing occlusion of downstream sites and promoting *FLO11* transcription. This interplay between Flo8 and Sfl1 is reminiscent of exclusive toggle switches in prokaryotes (54–56) where binding domains for transcription factors that control two adjacent operons overlap, such that only one factor can bind at a time. In such systems, binding competition determines which operon is exclusively transcribed. Competition between Sfl1 and Flo8 generates opposing outputs from the same regulatory region and forms the basis of an analogous switch between two transcriptional states. A similar configuration detected at the variegating *FLO10* locus (Fig. S3*B*) (35) supports this model.

This ncRNA circuitry helps to solve a puzzle concerning Rpd3L. This HDAC is a net activator of *FLO11*, a surprising role given its function in silencing other target genes (36–38). We propose that Rpd3L activates *FLO11* expression by having its anticipated role in condensing chromatin at a site far upstream of the *FLO11* core promoter. Localized chromatin condensation by Rpd3L at an upstream site could (*i*) hinder the access of Sfl1 to its binding site, but promote Flo8 binding (Fig. 5), and/or (*ii*) directly repress *ICR1* transcription, in either case toggling the *FLO11* promoter toward a state competent for transcription of the protein-coding ORF. Three results support a proposed role for Rpd3L. First, Rpd3L localizes to the same region (Fig. 2*A*) where Sfl1 and Flo8 bind (33, 57). Second, double mutant analysis suggests that Rpd3L's net-activation of *FLO11* occurs via inhibition of Sfl1-mediated repression: When Sfl1 function is lost, Rpd3L activity is not needed for transcription of *PWR1* (Fig. 3*D*) or *FLO11* (Fig. 1*A*). Third, if Rpd3L function normally hinders Sfl1 and/or promotes Flo8 binding, then Sfl1 would be expected to occupy its site more often and Flo8 less often (Fig. 2*B*) in an Rpd3L$^-$ mutant. When both Rpd3L and Sfl1 functions are lost, Flo8 could access its binding site more readily (Fig. 2*B*). However, we cannot exclude the possibility that up-regulation of *PWR1* itself in *sfl1* dominates over the repressive effects of increased *ICR1* when Rpd3L function is also lost, a consequence of the coupled regulation in this toggle switch. Weak Rpd3 localization detected ~2,850 bp upstream of *FLO11* (Fig. 2*A*) and the observation that *ICR1* transcription is lower in the *sfl1 flo8* double mutant compared with the Rpd3L$^-$ *sfl1 flo8* triple mutant (Fig. 3*D*) point to the possibility of some Sfl1-independent role for Rpd3L in repressing *ICR1* transcription.

ICR1 and *PWR1* are implicated in controlling an epigenetic phenomenon in yeast (35) that involves the reversible transition from a chromatin state that is competent for transcription of a protein-coding ORF to one that is silenced for its transcription. The roles proposed for these ncRNAs, which share features with mammalian lincRNAs (5), may have general significance for epigenetic regulation in other eukaryotes. There is evidence that epigenetic phenomena, such as imprinting and X-inactivation in mammals, involve ncRNAs (58). Our discovery of a circuitry involving two ncRNAs at the yeast *FLO11* locus suggests that regulation of other epigenetic phenomena that involve a progression from an unstable or bistable condition to a stable transcriptional state (either on or off) may, like the *FLO11* gene, be controlled by underlying ncRNA regulatory networks.

Materials and Methods

Strains, Media, Microbiological Techniques, and Growth Conditions. Yeast strains used in this study (Table S1) are derived from Σ1278b (28). Standard yeast media were prepared and genetic manipulation techniques were carried out as described (59). For experiments with P_{FLO11}-*URA3* strains, YPD liquid cultures were grown overnight, diluted 1:50, and grown to OD_{600} 0.8–1.2. Culture densities were adjusted to equivalence, serially diluted 4-fold, and spotted onto synthetic complete (SC), SC-Ura, and SC + 5-FOA (0.1%) agar plates (60). Haploid adhesion tests were performed as described (30). To induce pseudohyphal growth, strains were grown on SLAD media (61). For Northern blot analysis, qPCR, ChIP, RACE, and microarray expression analysis, cells were grown overnight in YPD liquid, diluted 1:50, and grown to OD_{600} 0.8–1.2 for use in experiments. Plasmids are listed in Table S1.

Northern Blot Analysis. For the Northern blot analysis in Fig. 1*B*, total RNA isolated by standard acid phenol extraction was used. For all other blots, total RNA was oligo(dT)-selected to enrich for polyadenylated transcripts. RNAs were separated on formaldehyde-agarose denaturing gels and blotted as described (62). Hybond membranes were hybridized with ^{32}P (exo-) Klenow-labeled DNA probes (Fig. 1*C* and load controls) or ^{32}P-labeled RNA probes generated with the Ambion T7 Maxiscript Kit (all other hybridizations).

ChIPs. Protocols have been described (63). Briefly, IPs were performed with Dynal Protein G magnetic beads preincubated with antibodies against Myc-epitope (Covance 9E-11 MMS-164P), yeast TBP (Santa Cruz SC-33736), or histone H4 (Upstate Millipore 05-858). For gene-specific ChIP, SYBR Green qPCR (Applied Biosystems) was performed on IP and WCE using specific primers. For ChIP-chip, Cy-5 labeled IP and Cy-3 WCE were hybridized to Σ1278b custom genomic microarrays (Agilent, strand-specific probes ~every 50 bp). Data were normalized as follows: Cross-talk normalization provided coefficients for Cy5→Cy3 and Cy3→Cy5 to correct intensities in each channel. Resulting values were median normalized. The data were transformed under the assumption that Cy3 = Cy5 is a good fit. JBD algorithm identified binding events (64).

qPCR. Total RNA obtained by standard acid phenol extraction was reversed transcribed (Qiagen QuantiTect Kit); cDNAs were analyzed with primers specific to targets, SYBR Green reagents (Applied Biosystems), and the ABI 7500 qPCR system.

Genome-Wide Transcription Profiling. Cy3- or Cy5-labeled cDNAs were generated using SuperScript II Reverse Transcriptase on Poly(A) RNA, hybridized to Σ1278b custom genomic microarrays (Agilent, strand-specific probes ~every 25 bp), and scanned (Agilent). Data were normalized as follows: Cross-talk normalization provided coefficients for Cy5→Cy3 and Cy3→Cy5 to correct intensities in each channel. Resulting values were median normalized. The data were trans-

formed under the assumption that Cy3 = Cy5 is a good fit. Differential expression between samples on the same array was determined as the difference in median intensity of the set of probes associated with a given transcript.

RACE. Mapping of 5′ and 3′ ends of capped, polyadenylated RNA was carried out with specific primers and the Invitrogen GeneRacer Kit. RACE products were cloned (pCR4-TOPO) and sequenced.

ACKNOWLEDGMENTS. We thank R. Young (Whitehead Institute) for reagents to generate Myc-tagged Rpd3; A. Rolfe and T. Danford for their contributions to design and analysis of the Σ1278b microarrays; O. Ryan and C. Boone (University of Toronto, Toronto) for their *rpd3*Δ strains; C. Wu (Whitehead Institute) for sharing strains yCW91 and yCW180 and primers CW352-CW355; and F. Lewitter for sharing bioinformatics expertise. This work was supported by National Institutes of Health Grants GM035010, 1R01GM069676, and DK076284 (to R.D.D.). G.R.F. is an American Cancer Society Professor.

1. Bertone P, et al. (2004) Global identification of human transcribed sequences with genome tiling arrays. *Science* 306:2242–2246.
2. David L, et al. (2006) A high-resolution map of transcription in the yeast genome. *Proc Natl Acad Sci USA* 103:5320–5325.
3. Davis CA, Ares M, Jr (2006) Accumulation of unstable promoter-associated transcripts upon loss of the nuclear exosome subunit Rrp6p in *Saccharomyces cerevisiae*. *Proc Natl Acad Sci USA* 103:3262–3267.
4. FANTOM Consortium (2005) The transcriptional landscape of the mammalian genome. *Science* 309:1559–1563.
5. Guttman M, et al. (2009) Chromatin signature reveals over a thousand highly conserved large noncoding RNAs in mammals. *Nature* 458:223–227.
6. Katayama S, et al. (2005) Antisense transcription in the mammalian transcriptome. *Science* 309:1564–1566.
7. Mercer TR, Dinger ME, Sunkin SM, Mehler MF, Mattick JS (2008) Specific expression of long noncoding RNAs in the mouse brain. *Proc Natl Acad Sci USA* 105:716–721.
8. Miura F, et al. (2006) A large-scale full-length cDNA analysis to explore the budding yeast transcriptome. *Proc Natl Acad Sci USA* 103:17846–17851.
9. Nagalakshmi U, et al. (2008) The transcriptional landscape of the yeast genome defined by RNA sequencing. *Science* 320:1344–1349.
10. Samanta MP, Tongprasit W, Sethi H, Chin CS, Stolc V (2006) Global identification of noncoding RNAs in *Saccharomyces cerevisiae* by modulating an essential RNA processing pathway. *Proc Natl Acad Sci USA* 103:4192–4197.
11. Steinmetz EJ, et al. (2006) Genome-wide distribution of yeast RNA polymerase II and its control by Sen1 helicase. *Mol Cell* 24:735–746.
12. Xu Z, et al. (2009) Bidirectional promoters generate pervasive transcription in yeast. *Nature* 457:1033–1037.
13. Neil H, et al. (2009) Widespread bidirectional promoters are the major source of cryptic transcripts in yeast. *Nature* 457:1038–1042.
14. Shamovsky I, Nudler E (2006) Gene control by large noncoding RNAs. *Sci STKE* pe40.
15. Prasanth KV, Spector DL (2007) Eukaryotic regulatory RNAs: An answer to the genome complexity conundrum. *Genes Dev* 21:11–42.
16. Lippman Z, Martienssen R (2004) The role of RNA interference in heterochromatic silencing. *Nature* 431:364–370.
17. Ponjavic J, Ponting CP, Lunter G (2007) Functionality or transcriptional noise? Evidence for selection within long noncoding RNAs. *Genome Res* 17:556–565.
18. Struhl K (2007) Transcriptional noise and the fidelity of initiation by RNA polymerase II. *Nat Struct Mol Biol* 14:103–105.
19. Panning B, Dausman J, Jaenisch R (1997) X chromosome inactivation is mediated by Xist RNA stabilization. *Cell* 90:907–916.
20. Sheardon SA, et al. (1997) Stabilization of Xist RNA mediates initiation of X chromosome inactivation. *Cell* 91:99–107.
21. Amrein H, Axel R (1997) Genes expressed in neurons of adult male *Drosophila*. *Cell* 88:459–469.
22. Meller VH, Wu KH, Roman G, Kuroda MI, Davis RL (1997) roX1 RNA paints the X chromosome of male *Drosophila* and is regulated by the dosage compensation system. *Cell* 88:445–457.
23. Martens JA, Laprade L, Winston F (2004) Intergenic transcription is required to repress the *Saccharomyces cerevisiae* SER3 gene. *Nature* 429:571–574.
24. Martens JA, Wu PY, Winston F (2005) Regulation of an intergenic transcript controls adjacent gene transcription in *Saccharomyces cerevisiae*. *Genes Dev* 19:2695–2704.
25. Hongay CF, Grisafi PL, Galitski T, Fink GR (2006) Antisense transcription controls cell fate in *Saccharomyces cerevisiae*. *Cell* 127:735–774.
26. Camblong J, Iglesias N, Fickentscher C, Dieppois G, Stutz F (2007) Antisense RNA stabilization induces transcriptional gene silencing via histone deacetylation in *S. cerevisiae*. *Cell* 131:706–717.
27. Uhler JP, Hertel C, Svejstrup JQ (2007) A role for noncoding transcription in activation of the yeast PHO5 gene. *Proc Natl Acad Sci USA* 104:8011–8016.
28. Liu H, Styles CA, Fink GR (1996) *Saccharomyces cerevisiae* S288C has a mutation in FLO8, a gene required for filamentous growth. *Genetics* 144:967–978.
29. Pan X, Heitman J (1999) Cyclic AMP-dependent protein kinase regulates pseudohyphal differentiation in *Saccharomyces cerevisiae*. *Mol Cell Biol* 19:4874–4887.
30. Guo B, Styles CA, Feng Q, Fink GR (2000) A *Saccharomyces* gene family involved in invasive growth, cell-cell adhesion, and mating. *Proc Natl Acad Sci USA* 97:12158–12163.
31. Conlan RS, Tzamarias D (2001) Sfl1 functions via the co-repressor Ssn6-Tup1 and the cAMP-dependent protein kinase Tpk2. *J Mol Biol* 309:1007–1015.
32. Reynolds TB, Fink GR (2001) Bakers' yeast, a model for fungal biofilm formation. *Science* 291:878–881.
33. Pan X, Heitman J (2002) Protein kinase A operates a molecular switch that governs yeast pseudohyphal differentiation. *Mol Cell Biol* 22:3981–3993.
34. Palecek SP, Parikh AS, Kron SJ (2002) Sensing, signalling and integrating physical processes during *Saccharomyces cerevisiae* invasive and filamentous growth. *Microbiology* 148:893–907.
35. Halme A, Bumgarner S, Styles C, Fink GR (2004) Genetic and epigenetic regulation of the FLO gene family generates cell-surface variation in yeast. *Cell* 116:405–415.
36. Carrozza MJ, et al. (2005) Stable incorporation of sequence specific repressors Ash1 and Ume6 into the Rpd3L complex. *Biochim Biophys Acta* 1731:77–87.
37. Kadosh D, Struhl K (1997) Repression by Ume6 involves recruitment of a complex containing Sin3 corepressor and Rpd3 histone deacetylase to target promoters. *Cell* 89:365–371.
38. Rundlett SE, Carmen AA, Suka N, Turner BM, Grunstein M (1998) Transcriptional repression by UME6 involves deacetylation of lysine 5 of histone H4 by RPD3. *Nature* 392:831–835.
39. De Nadal E, et al. (2004) The MAPK Hog1 recruits Rpd3 histone deacetylase to activate osmoresponsive genes. *Nature* 427:370–374.
40. Sertil O, Vemula A, Salmon SL, Morse RH, Lowry CV (2007) Direct role for the Rpd3 complex in transcriptional induction of the anaerobic DAN/TIR genes in yeast. *Mol Cell Biol* 27:2037–2047.
41. Sharma VM, Tomar RS, Dempsey AE, Reese JC (2007) Histone deacetylases RPD3 and HOS2 regulate the transcriptional activation of DNA damage-inducible genes. *Mol Cell Biol* 27:3199–3210.
42. Xin X, Lan C, Lee HC, Zhang L (2007) Regulation of the HAP1 gene involves positive actions of histone deacetylases. *Biochem Biophys Res Commun* 362:120–125.
43. Carrozza MJ, et al. (2005) Histone H3 methylation by Set2 directs deacetylation of coding regions by Rpd3S to suppress spurious intragenic transcription. *Cell* 123:581–592.
44. Robertson LS, Fink GR (1998) The three yeast A kinases have specific signaling functions in pseudohyphal growth. *Proc Natl Acad Sci USA* 95:13783–13787.
45. Robert F, et al. (2004) Global position and recruitment of HATs and HDACs in the yeast genome. *Mol Cell* 16:199–209.
46. Grunstein M (1997) Histone acetylation in chromatin structure and transcription. *Nature* 389:349–352.
47. Gueldener U, Heinisch J, Koehler GJ, Voss D, Hegemann JH (2002) A second set of loxP marker cassettes for Cre-mediated multiple gene knockouts in budding yeast. *Nucleic Acids Res* 30:e23.
48. Güldener U, Heck S, Fiedler T, Beinhauer J, Hegemann JH (1996) A new efficient gene disruption cassette for repeated use in budding yeast. *Nucleic Acids Res* 24:2519–2524.
49. Karolchik D, et al. (2008) The UCSC Genome Browser Database: 2008 update. *Nucleic Acids Res* 36:D773–D779.
50. Kellis M, Patterson N, Endrizzi M, Birren B, Lander ES (2003) Sequencing and comparison of yeast species to identify genes and regulatory elements. *Nature* 423:241–254.
51. Galitski T, Saldanha AJ, Styles CA, Lander ES, Fink GR (1999) Ploidy regulation of gene expression. *Science* 285:251–254.
52. Mumberg D, Muller R, Funk M (1995) Yeast vectors for the controlled expression of heterologous proteins in different genetic backgrounds. *Gene* 156:119–122.
53. Rupp S, Summers E, Lo HJ, Madhani H, Fink G (1999) MAP kinase and cAMP filamentation signaling pathways converge on the unusually large promoter of the yeast FLO11 gene. *EMBO J* 18:1257–1269.
54. Ptashne M (1992) *A Genetic Switch: Phage Lambda and Higher Organisms* (Blackwell Science and Cell Press, Oxford), 2nd Ed.
55. Wagner R (2000) *Transcription Regulation in Prokaryotes* (Oxford Univ Press, Oxford).
56. Warren PB, Wolde PR (2004) Enhancement of the stability of genetic switches by overlapping upstream regulatory domains. *Phys Rev Lett* 92:128101.
57. Borneman AR, et al. (2006) Target hub proteins serve as master regulators of development in yeast. *Genes Dev* 20:435–448.
58. Pauler FM, Koerner MV, Barlow DP (2007) Silencing by imprinted noncoding RNAs: Is transcription the answer? *Trends Genet* 23:284–292.
59. Guthrie C, Fink GR (2001) Guide to yeast genetics and molecular and cellular biology. *Methods Enzymol* 350–351.
60. Boeke JD, Trueheart J, Natsoulis G, Fink GR (1987) 5-Fluoroorotic acid as a selective agent in yeast molecular genetics. *Methods Enzymol* 154:164–175.
61. Gimeno CJ, Ljungdahl PO, Styles CA, Fink GR (1992) Unipolar cell divisions in the yeast *S. cerevisiae* lead to filamentous growth: Regulation by starvation and RAS. *Cell* 68:1077–1090.
62. Sambrook J, Fritsch EF, Maniatis T (1989) *Molecular Cloning: A Laboratory Manual* (Cold Spring Harbor Lab Press, Plainview, NY), 2nd Ed.
63. Lee TI, Johnstone SE, Young RA (2006) Chromatin immunoprecipitation and microarray-based analysis of protein location. *Nat Protocols* 1:729–748.
64. Qi Y, et al. (2006) High-resolution computational models of genome binding events. *Nat Biotech* 24:963–970.